CONF-850507--27

RECEIVED BY OSTI JUN 07 1985

LA-UR--85-1731

DE85 012727

Los Alamos National Laboratory is operated by the University of California for the United States Department of Energy under contract W-7405-ENG-36

TITLE. EFFECT OF FISSION DYNAMICS ON THE SPECTRA AND MULTIPLICITIES OF PROMPT FISSION NEUTRONS

AUTHOR(S). J. Ray[illegible]d Nix, David G. Madland, and Arnold J. Sierk

SUBMITTED TO. for presentation at the International Conference on Nuclear Data for Basic and Applied Science, Santa Fe, New Mexico May 13-17, 1985

DISCLAIMER

MASTER

Los Alamos Los Alamos National Laboratory
Los Alamos, New Mexico 87545

EFFECT OF FISSION DYNAMICS ON THE SPECTRA AND MULTIPLICITIES OF PROMPT FISSION NEUTRONS

J. Rayford Nix, David G. Madland, and Arnold J. Sierk

May 10, 1985

For presentation at the International Conference on
Nuclear Data for Basic and Applied Science,
Santa Fe, New Mexico, May 13-17, 1985

EFFECT OF FISSION DYNAMICS ON THE SPECTRA AND MULTIPLICITIES OF PROMPT FISSION NEUTRONS

J. RAYFORD NIX, DAVID G. MADLAND, AND ARNOLD J. SIERK
Theoretical Division, Los Alamos National Laboratory, Los Alamos, New Mexico 87545, U.S.A.

Abstract With the goal of examining their effect on the spectra and multiplicities of the prompt neutrons emitted in fission, we discuss recent advances in a unified macroscopic-microscopic description of large-amplitude collective nuclear dynamics. The conversion of collective energy into single-particle excitation energy is calculated for a new surface-plus-window dissipation mechanism. By solving the Hamilton equations of motion for initial conditions appropriate to fission, we obtain the average fission-fragment translational kinetic energy and excitation energy. The spectra and multiplicities of the emitted neutrons, which depend critically upon the average excitation energy, are then calculated on the basis of standard nuclear evaporation theory, taking into account the average motion of the fission fragments, the distribution of fission-fragment residual nuclear temperature, the energy dependence of the cross section for the inverse process of compound-nucleus formation, and the possibility of multiple-chance fission. Some illustrative comparisons of our calculations with experimental data are shown.

INTRODUCTION

The renaissance in fission theory that began two decades ago has contributed substantially to our understanding and tabulation of nuclear data for basic and applied science, as well as to our ability to calculate relevant quantities when they cannot be measured experimentally. This renaissance started with the development by Strutinsky,[1] following work by Swiatecki[2] and others, of a new macroscopic-microscopic method for calculating the potential energy of a nucleus as a function of its shape. This method synthesizes the best features of two complementary approaches, taking the smooth trends of the potential energy from a macroscopic model and the local fluctuations from a microscopic model.[3] Fission barriers calculated with this method provided a natural interpretation of such diverse experimental phenomena as spontaneously fis-

sioning isomers, resonances in fission cross sections, and asymmetric fission-fragment mass distributions.[4]

From such static potential-energy calculations of fission barriers, attention turned later to dynamical aspects of collective nuclear motion. The determination of the magnitude and mechanism of nuclear dissipation has proved a difficult challenge, but with the help of new experimental clues provided by giant resonances, fission, and heavy-ion reactions, we have just gained some new insight into this problem. Our new picture of nuclear dissipation provides a unified macroscopic description for nuclei throughout the periodic table of such diverse phenomena as the widths of isoscalar giant quadrupole and giant octupole resonances, average fission-fragment kinetic energies and excitation energies, and widths of charge and mass distributions in deep-inelastic heavy-ion reactions.

To adequately describe our new dissipation picture, we need first to review the macroscopic-microscopic method that provides the basis for our dynamical calculations. We will then present some results that have just been calculated with this new dissipation picture, including average fission-fragment kinetic energies for the fission of nuclei throughout the periodic table. These are necessary for the calculation of the spectra and average multiplicities of the prompt neutrons emitted in fission, to which we turn our attention in the second part of the paper.

MACROSCOPIC-MICROSCOPIC METHOD

For a system of A nucleons, we separate the 3A degrees of freedom representing their center-of-mass motion into N collective degrees of freedom that are treated explicitly and 3A - N internal degrees of freedom that are treated implicitly. For our present fission calculations, which are restricted to axially symmetric and mass-symmetric shapes, we choose our N collective coordinates $q_1, \ldots, q_N = q$ as the coefficients of even Legendre polynomials $P_{2n}(z/z_0)$ in an expansion in cylindrical coordinates of the square of the perpendicular distance from the symmetry axis z to the nuclear surface, where z_0 is one-half the distance between the two ends of the shape.[5] The present results are calculated with N = 5.

Potential Energy

We consider excitation energies $E^* \gtrsim 50$ MeV, where single-particle effects may be neglected, and calculate the potential energy of deformation V(q) as the sum of a repulsive Coulomb energy and an attractive Yukawa-plus-exponential potential.[6] This generalized surface energy takes into account the reduction in energy arising from the nonzero range of the nuclear force in such a way that saturation is ensured for two semi-infinite slabs in contact.

Kinetic Energy

The collective kinetic energy is a quadratic function of the collective velocities $\dot{q}$, with coefficients that are related to the elements of the shape-dependent inertia tensor M(q). At the high excitation energies and large deformations considered here, where pairing correlations have disappeared and near crossings of single-particle levels have become less frequent, the vibrational inertia is close to the incompressible, irrotational value.[7] We calculate the inertia tensor M(q) for incompressible, nearly irrotational flow by use of the Werner-Wheeler method, which determines the flow in terms of circular layers of fluid.[8]

Dissipation Mechanism

The coupling between the collective and internal degrees of freedom gives rise to a dissipative force whose mean component in the i-th direction may be written as

$$F_i = - \eta_{ij}(q)\, \dot{q}_j \quad , \tag{1}$$

with the convention that repeated indices are to be summed over from 1 to N. For the calculation of the shape-dependent dissipation tensor $\eta(q)$ that describes the conversion of collective energy into internal single-particle excitation energy, we introduce a new surface-plus-window mechanism that involves interactions of either one or two nucleons with the moving nuclear surface and also, for dumbbell-like shapes encountered in fission and heavy-ion reactions, the transfer of nucleons through the window separating the two portions of the system. This novel dissipation mechanism is a consequence of the Pauli exclusion principle for fermions, which gives the nucleons inside a nucleus a mean free path that is long compared to the nuclear radius, so that collisions between nucleons in the nuclear interior are rare.

For the surface part of the dissipation, the leading term in an expansion of the time rate of change of the collective Hamiltonian H can be written in terms of an integral over the nuclear surface as[9]

$$\frac{dH}{dt} = - k_s\, \rho \bar{v} \int (\dot{n} - D)^2\, dS = -2R \quad , \tag{2}$$

where $\dot{n}$ is the velocity of a surface element dS, D is the normal drift velocity of nucleons about to strike the surface element dS, $\bar{v}$ is the average speed of the nucleons inside the nucleus, ρ is the nuclear mass density, and k_s is a dimensionless parameter that specifies the total strength of the interaction of either one or two nucleons with the moving nuclear surface. A value of $k_s = 1$

would correspond to the classical wall formula of Swiatecki,[9] but we obtain here the much smaller value of $k_s = 0.27$ by adjustment to experimental widths of isoscalar giant quadrupole and giant octupole resonances.[10] This substantial reduction in the value of k_s arises from a breakdown of the randomization assumption inherent in the wall formula, as well as from the effects of replacing three additional idealizations of the wall formula by more realistic features appropriate to real nuclei.[11] In terms of the Rayleigh dissipation function R defined by Eq. (2), the force F_i arising from the surface part of the dissipation is given by $F_i = - \partial R/\partial \dot{q}_i$.

For dumbbell-like shapes, the transfer of nucleons through the window separating the two portions of the system leads to an additional dissipation that is given by the classical window formula of Swiatecki.[9] There is no need to renormalize this part of the dissipation because nucleons that have passed through a small window have a low probability of returning through it while still retaining memory of their previous passage. To describe the transition from the pure surface dissipation that applies to mononuclear shapes, where the drift D is zero in Eq. (2), to the surface-plus-window dissipation that applies to dinuclear shapes, where the drift D is nonzero in Eq. (2), we use a smooth interpolation analogous to that used in Ref. 12.

Equations of Motion

In addition to the mean dissipative force, the coupling between the collective and internal degrees of freedom gives rise to a residual fluctuating force, which we treat under the Markovian assumption that it does not depend upon the system's previous history. At high excitation energies, where classical statistical mechanics is valid, we are led to a generalized Fokker-Planck equation for the dependence upon time t of the distribution function $f(q,p,t)$ in phase space of collective coordinates and momenta.[12] In our studies here we use equations for the time rate of change of the first moments of the distribution function, with the neglect of higher moments. These are the generalized Hamilton equations,[12] which we solve numerically for each of the N generalized coordinates and momenta.

DYNAMICAL FISSION CALCULATIONS

We show in Figure 1 how our new surface-plus-window dissipation, with strength $k_s = 0.27$, slows down the dynamical evolution of an excited ^{240}Pu nucleus compared to that for no dissipation. The initial conditions at the fission saddle point incorporate the effect of dissipation on the fission direction and are calculated

for a nuclear temperature of 2 MeV by determining the mean velocity of all nuclei that pass per unit time through the saddle point with positive velocity.[12] Compared to the values for no dissipation, surface-plus-window dissipation increases the time from the saddle point to a zero-neck-radius scission point from 2.6×10^{-21} s to 8.6×10^{-21} s, and decreases the translational kinetic energy at scission from 50.0 MeV to 12.9 MeV. Leading to a scission shape that is more compact than that for no dissipation, surface-plus-window dissipation gives 27.9 MeV of dissipated energy during the dynamical descent from saddle to scission.

We treat the post-scission dynamical motion in terms of two spheroids, with initial conditions determined by keeping continuous the values of two shape moments and their time derivatives. Surface-plus-window dissipation reduces the average fission-fragment translational kinetic energy at infinity from 193.6 MeV for no dissipation to 177.1 MeV.

Our calculated average kinetic energies for the fission of nuclei throughout the periodic table, with the atomic number Z

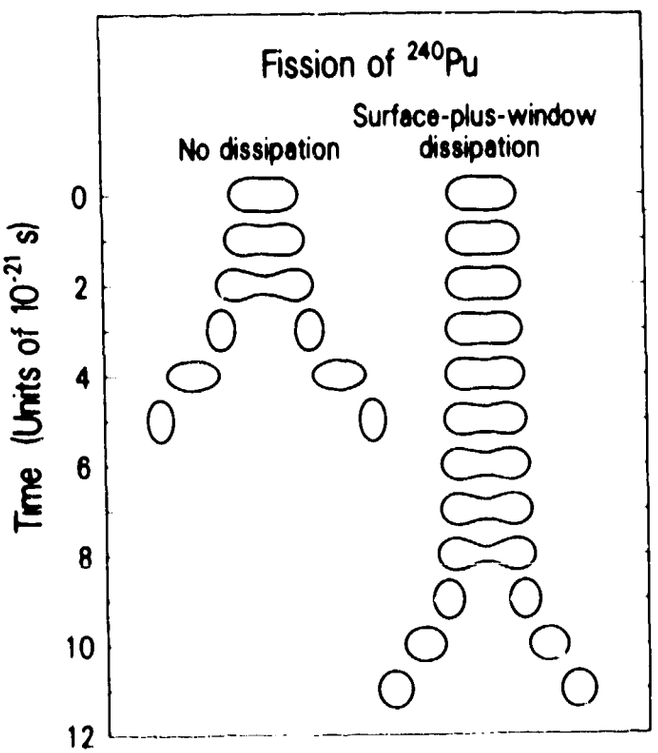

FIGURE 1 Effect of surface-plus-window dissipation on the dynamical evolution of ^{240}Pu beyond its fission saddle point, for a nuclear temperature of 2 MeV.

related to the mass number A according to Green's approximation to the valley of beta stability,[13] are shown in Figure 2 for a nuclear temperature of 2 MeV. When compared with experimental values for the fission of nuclei at high excitation energy,[12] where single-particle effects have decreased in importance, the dashed curves calculated with no dissipation are for heavy nuclei substantially higher. The presence of two dashed curves for $Z^2/A^{1/3} \geq 1500$ results from our use of two different approximations for treating the post-scission motion when a third fragment has formed between the two end fragments.[12] The solid curve, calculated with our new surface-plus-window dissipation with a strength previously determined from the widths of isoscalar giant resonances, satisfactorily reproduces the experimental data, although it lies slightly above some of the data for $Z^2/A^{1/3} \cong 1300$ and slightly below for $Z^2/A^{1/3} \geq 1900$. These small discrepancies could be associated with effects arising from the rupture of the neck prior to its reaching a zero radius, as is currently required in our calculations.

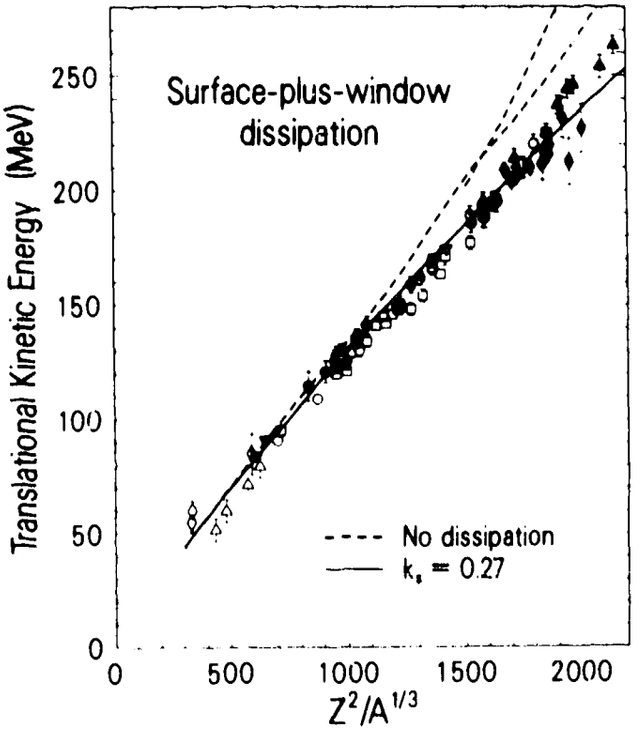

FIGURE 2 Reduction of average fission-fragment kinetic energies by surface-plus-window dissipation, compared to experimental values.

PROMPT FISSION NEUTRON SPECTRUM

By use of the above dynamical calculations, with dissipation described by our new surface-plus-window mechanism, we can now determine for high-excitation fission that portion of the available energy that on the average goes into translational kinetic energy of the fission fragments. Although analogous dynamical calculations have not yet been performed for low-excitation fission, where the nuclear potential energy, inertia, and dissipation are all affected by single-particle shell and pairing effects, the average fission-fragment kinetic energy can in some cases be obtained directly from experimental measurements and in other cases from least-squares adjustments to nearby systems.[14] The remaining portion of the available energy goes into fragment excitation energy, which is dissipated primarily by the emission of neutrons and gamma rays. The spectra and multiplicities of the emitted neutrons are required for many applications, and we now turn to their calculation, for which purpose we use standard nuclear evaporation theory.

As discussed in detail in Ref. 15, we take into account the average motion of the fission fragments from which the neutrons are emitted, the distribution of fission-fragment residual nuclear temperature resulting from fragment cooling as neutrons are emitted, the energy dependence of the cross section for the inverse process of compound-nucleus formation, and effects arising from the possibility of multiple-chance fission.

In the center-of-mass system of a given fission fragment, the neutron energy spectrum corresponding to a fixed residual nuclear temperature T is given approximately by[16]

$$\phi(\varepsilon) = k(T)\, \sigma_c(\varepsilon)\, \varepsilon \exp(-\varepsilon/T) \quad , \tag{3}$$

where ε is the center-of-mass neutron energy, $\sigma_c(\varepsilon)$ is the cross section for the inverse process of compound-nucleus formation, and $k(T)$ is a temperature-dependent normalization constant, determined so that unity is obtained when Eq. (3) is integrated over energy from zero to infinity.

We approximate the distribution of fission-fragment residual nuclear temperature[17] by a right-triangular distribution up to a maximum temperature T_m, which is related to the initial total average fission-fragment excitation energy $\langle E^* \rangle$ and the nuclear level-density parameter a by $T_m = (\langle E^* \rangle / a)^{1/2}$. The average excitation energy is in turn given by

$$\langle E^* \rangle = \langle E_r \rangle + B_n + E_n - \langle E_k \rangle \quad , \tag{4}$$

where $\langle E_r \rangle$ is the average energy relase, B_n and E_n are the separa-

tion energy and kinetic energy of the neutron inducing fission, and $\langle E_k \rangle$ is the total average fission-fragment kinetic energy. For spontaneous fission, both B_n and E_n in Eq. (4) are zero.

Equation (3) is next integrated over this right-triangular temperature distribution to yield the neutron energy spectrum in the center-of-mass system of a given fission fragment. This result is then transformed to the laboratory system under the assumption that the neutrons are emitted isotropically from each fission fragment,[17] whose average kinetic energy is obtained by momentum conservation from the average mass numbers of the light and heavy fragments and the total average kinetic energy. The laboratory prompt fission neutron spectrum N(E), where E is the neutron energy in the laboratory system, is given finally as the average of the laboratory spectra for the light and heavy fragments.[15]

For the special case in which the compound-nucleus cross section $\sigma_c(\varepsilon)$ is assumed constant, the laboratory spectrum N(E) can be expressed in closed form in terms of exponential integrals and incomplete gamma functions.[15] However, for most of our studies we calculate the energy dependence of $\sigma_c(\varepsilon)$ by use of the optical-model potential of Becchetti and Greenless,[18] in which case N(E) must be evaluated by numerical quadrature.

Figure 3 shows the resulting prompt fission neutron spectra N(E) for the fission of ^{235}U induced by 0.53-MeV neutrons, calculated for a constant cross section σ_c and an energy-dependent

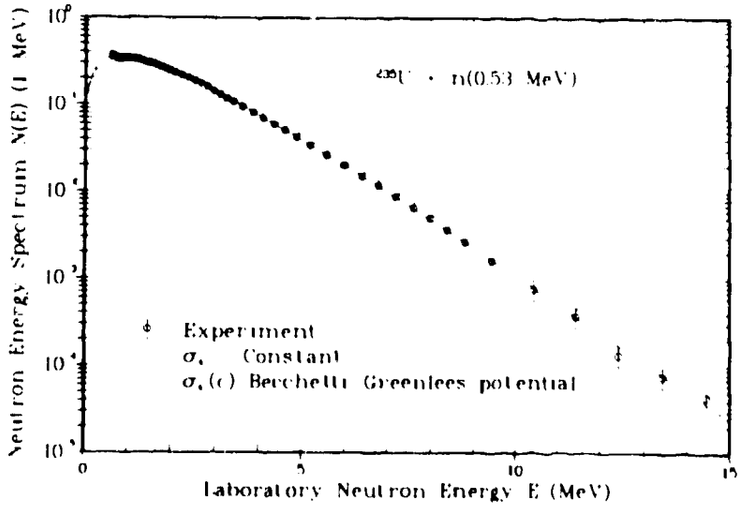

FIGURE 3 Comparison of calculated prompt fission neutron spectra with experimental values.

cross section $\sigma_c(\varepsilon)$. We also include the experimental data of Johansson and Holmqvist.[19] To accentuate the differences between the two calculations, we divide the calculation with an energy-dependent cross section and the experimental data by the calculation with a constant cross section and present the resulting ratios in Figure 4. For neutron energies $E \gtrsim 2$ MeV, both the experimental data and the calculation with an energy-dependent cross section lie below the calculation with a constant cross section, by up to about 25%. Conversely, for $E \lesssim 2$ MeV, both the experimental data and the calculation with an energy-dependent cross section lie above the calculation with a constant cross section, by up to about 10%. This comparison demonstrates the importance of taking into account the energy dependence of $\sigma_c(\varepsilon)$ when calculating N(E). This energy dependence is taken into account in our calculations of the ^{252}Cf spontaneous-fission standard reaction presented elsewhere in this Conference.[20]

Our approach permits the calculation of N(E) as a function of both the fissioning nucleus and the incident neutron energy E_n. When E_n is larger than about 6 MeV, fission is possible following the emission of one or more neutrons. Effects arising from such multiple-chance-fission processes can be taken into account by considering a superposition of spectra, weighted according to the appropriate fission probabilities.[15]

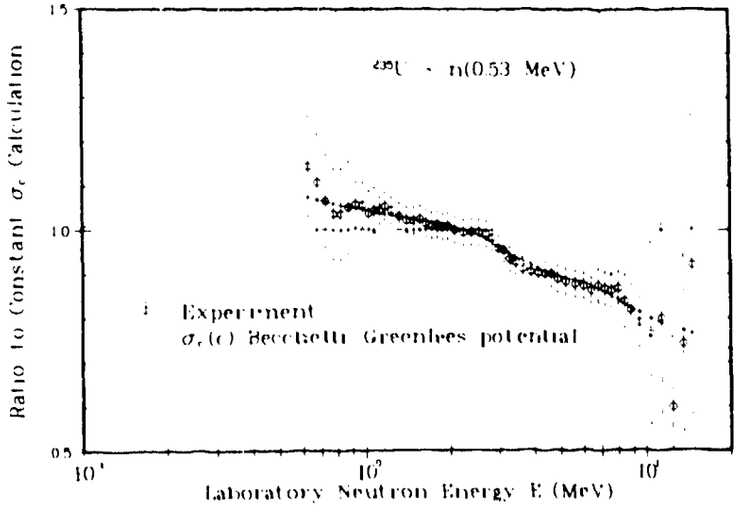

FIGURE 4 Detailed comparison with experimental values, showing the effect of the energy dependence of the compound-nucleus-formation cross section on the prompt fission neutron spectrum.

AVERAGE PROMPT NEUTRON MULTIPLICITY

For first-chance fission, the average total number of prompt neutrons emitted per fission is given approximately by the total average energy available for neutron emission divided by the average energy removed per emitted neutron. The resulting equation is[15]

$$\bar{\nu}_p = (\langle E^* \rangle - \langle E_\gamma \rangle)/(\langle S_n \rangle + \langle \varepsilon \rangle) \quad , \tag{5}$$

where $\langle E_\gamma \rangle$ is the total average prompt gamma-ray energy per fission, $\langle S_n \rangle$ is the average fission-fragment neutron separation energy, and $\langle \varepsilon \rangle$ is the average center-of-mass energy of the emitted neutrons. The total average excitation energy $\langle E^* \rangle$ is given by Eq. (4). For multiple-chance fission, a superposition of expressions like Eq. (5), weighted according to the appropriate fission probabilities, can be used.[15]

For the neutron-induced fission of ^{235}U, Figure 5 compares our predictions for the average prompt neutron multiplicity as a function of incident neutron energy with experimental values.[15] The solid curve, which includes the effects of multiple-chance fission, reproduces the measurements with better than 1% accuracy for thermal neutron energies up to 0.5 MeV, and with about 2% accuracy for neutron energies between 6 and 15 MeV. However, for

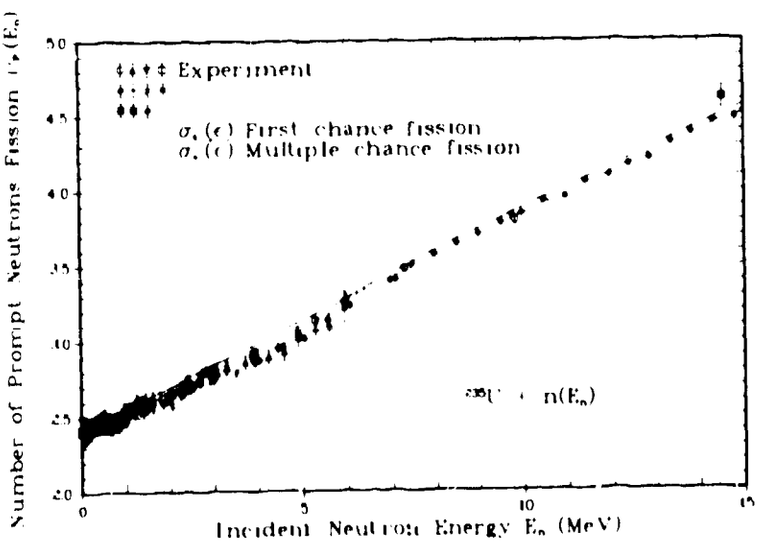

FIGURE 5 Effect of multiple-chance fission on the average prompt neutron multiplicity as a function of the incident neutron energy, compared to experimental values.

neutron energies near 4.5 MeV, the calculations are about 4% higher than the measurements. This discrepancy probably arises from our neglect of the dependencies of $\langle E_r \rangle$, $\langle S_n \rangle$, $\langle E_k \rangle$, and $\langle E_\gamma \rangle$ on the incident neutron energy. For this system, multiple-chance fission introduces a small upward step at the second-chance fission threshold near 5.5 MeV, which is evident in the experimental data, and a very small downward step at the third-chance fission threshold near 12 MeV. The effects of multiple-chance fission are larger for some other fissioning systems.

SCISSION NEUTRONS

In our calculations of the prompt fission neutron spectrum and average prompt neutron multiplicity, we have thus far neglected any effects arising from neutrons emitted dynamically in the neck region during scission. Angular distributions of the neutrons observed in the spontaneous fission[21] of ^{252}Cf and the thermal-neutron-induced fission[22] of ^{235}U have been analyzed in terms of an assumed isotropic component in the laboratory system to supplement the components arising from the moving fragments. In both cases these analyses gave an isotropic component in the laboratory system of about 10%, but because scission neutrons that are ejected dynamically from the neck would be emitted preferentially at 90° relative to the direction of the fission fragments rather than isotropically in the laboratory system, the actual fraction of scission neutrons should be less than 10%. With the aid of dynamical calculations like those in Figure 1 to give the speed and shape of the system near scission, one should be able to properly incorporate the effects of scission neutrons into our calculations of the prompt fission neutron spectrum and average prompt neutron multiplicity.

CONCLUSION

Starting two decades ago with the development of the static macroscopic-microscopic method, the renaissance in fission theory has now turned to dynamical aspects of collective nuclear motion. With a novel surface-plus-window dissipation mechanism, we are now able to perform dynamical calculations at high excitation energy for such quantities as the average fission-fragment kinetic energy and the speed and shape of the system near scission. Fundamental input of this type has made possible the accurate calculation of the prompt fission neutron spectrum and average prompt neutron multiplicity as functions of the fissioning nucleus and its excitation energy. Similar fundamental input is essential if we are to make further advances in our treatment of nuclear data for basic and applied science.

ACKNOWLEDGMENTS

We are grateful to J. J. Griffin and J. B. Wilhelmy for discussions that contributed to the development of our new surface-plus-window dissipation mechanism, and to F. E. Bertrand for making his new graphs of isoscalar giant multipole widths available to us prior to their publication. This work was supported by the U. S. Department of Energy.

REFERENCES

1. V. M. Strutinsky, Yad. Fiz., 3, 614 (1966); Sov. J. Nucl. Phys., 3, 449 (1966).
2. W. J. Swiatecki, in Proc. Second Int. Conf. on Nuclidic Masses, Vienna, 1963 (Springer-Verlag, Vienna, 1964), p. 58.
3. J. R. Nix, Annu. Rev. Nucl. Sci., 22, 65 (1972).
4. P. Möller and J. R. Nix, in Proc. Third IAEA Symp. on the Physics and Chemistry of Fission, Rochester, 1973 (International Atomic Energy Agency, Vienna, 1974), Vol. I, p. 103.
5. S. Trentalange, S. E. Koonin, and A. J. Sierk, Phys. Rev., C22, 1159 (1980).
6. P. Möller and J. R. Nix, Nucl. Phys., A361, 117 (1981).
7. J. Kunz and J. R. Nix, Z. Phys., to be published.
8. J. R. Nix, Nucl. Phys., A130, 241 (1969).
9. W. J. Swiatecki, Prog. Part. Nucl. Phys., 4, 383 (1980).
10. F. E. Bertrand, Nucl. Phys., A354, 129c (1981).
11. J. J. Griffin and M. Dworzecka, Phys. Lett., to be published.
12. J. R. Nix and A. J. Sierk, in Proc. Int. Conf. on Nuclear Physics, Bombay, 1984, to be published.
13. A. E. S. Green, Nuclear Physics (McGraw-Hill, New York, 1955), pp. 185, 250.
14. J. P. Unik, J. E. Gindler, L. E. Glendenin, K. F. Flynn, A. Gorski, and R. K. Sjoblom, in Proc. Third IAEA Symp. on the Physics and Chemistry of Fission, Rochester, 1973 (International Atomic Energy Agency, Vienna, 1974), Vol. II, p. 19.
15. D. G. Madland and J. R. Nix, Nucl. Sci. Eng., 81, 213 (1982).
16. V. F. Weisskopf, Phys. Rev., 52, 295 (1937).
17. J. Terrell, Phys. Rev., 113, 527 (1959).
18. F. D. Becchetti, Jr. and G. W. Greenlees, Phys. Rev., 182, 1190 (1969).
19. P. I. Johansson and B. Holmqvist, Nucl. Sci. Eng., 62, 695 (1977).
20. D. G. Madland, R. J. LaBauve, and J. R. Nix, in these Proceedings.
21. H. R. Bowman, S. G. Thompson, J. C. D. Milton, and W. J. Swiatecki, Phys. Rev., 126, 2120 (1962).
22. S. S. Kapoor, R. Ramanna, and P. N. Rama Rao, Phys. Rev., 131, 283 (1963).